Rheol Acta
DOI 10.1007/s00397-014-0776-0

ORIGINAL CONTRIBUTION

Capillary-driven percolating networks in ternary blends of immiscible polymers and silica particles

Trystan Domenech · Sachin Velankar

Received: 4 February 2014 / Revised: 4 April 2014 / Accepted: 7 April 2014

Abstract We investigate the structure and rheology of a melt-blended ternary system composed of a continuous polymer phase, silica particles in the few-micron size range, and a small amount of a second immiscible polymer phase which preferentially wets the particles. The morphology of the ternary system is found to consist of a volume-spanning "pendular network" of particles bridged by menisci of the wetting polymer, as well as "capillary aggregates" which are large compact particle aggregates saturated by the wetting polymer. The ternary blends have strongly non-Newtonian melt rheology due to the pendular network. The relative extent of capillary aggregation depends on the melt-blending history, and the rheological properties can be used to track the changes in the blend structure. The pendular network is seen at a particle loading of only 10 vol.%, demonstrating that capillary bridging lowers the percolation threshold of a particle-filled polymer.

Keywords Capillary bridging · Percolation · Pendular network · Ternary blends

Introduction

Addition of small amounts interfacially active particles into immiscible polymer blends during melt processing can have a significant effect on the multiphase morphology. For instance, in blends with a droplet–matrix morphology, the incorporation of interfacially active particles can sharply reduce the size of the dispersed phase (Baudouin et al. 2011; Elias et al. 2007; Fenouillot et al. 2009; Hong et al. 2006; Huitric et al. 2009; Ray et al. 2004; Si et al. 2006; Thareja et al. 2010; Vermant et al. 2004), analogous to the action of conventional compatibilizers (Van Puyvelde et al. 2001). Particles can also limit the coarsening of co-continuous morphologies in polymer blends with nearly equal volume fractions of the immiscible polymers (Gubbels et al. 1994). Similar arrest of coarsening of a two-phase co-continuous morphology has also been noted in polymer thin films (Chung et al. 2005) undergoing spinodal decomposition. Many of these morphological consequences of adding particles are attributable to the fact that particles can adsorb at the interface at a sufficiently high coverage to jam the interface into a solid-like state. Previous research has also revealed a different mechanism, viz. particle bridging across drops as another mechanism for morphological stabilization (Nagarkar and Velankar 2013, Nagarkar and Velankar 2012, Thareja and Velankar 2007, Vermant et al. 2008). Incidentally, much research on small-molecule oil–water systems with interfacially active particles has explored some of the same issues: particle-stabilized Ramsden–Pickering emulsions (Binks and Horozov 2006, Pickering 1907, Ramsden 1903), particle-stabilized co-continuous bijel morphologies (Cates and Clegg 2008, Herzig et al. 2007, Lee and Mohraz 2010, Witt et al. 2013), and particle-bridged emulsion structures (Horozov and Binks 2006, Lee et al. 2012, Stancik and Fuller 2004); each of which is analogous to the various multiphase polymer morphologies mentioned above and has been studied heavily in the last 15 years.

These results then pose an intriguing question: if a small amount of particulates added to a two-phase immiscible polymer blend can have large consequences, is the reverse also true? Can the addition of a small amount of immiscible polymer to a particle-filled polymer have similarly large consequences? Research addressing this question in small

Electronic supplementary material The online version of this article (doi:10.1007/s00397-014-0776-0) contains supplementary material, which is available to authorized users.

T. Domenech · S. Velankar (✉)
Department of Chemical Engineering, University of Pittsburgh, Pittsburgh, PA 15261, USA
e-mail: velankar@pitt.edu

Published online: 18 June 2014

molecule systems shows some remarkable results: the addition of a small amount of a second immiscible fluid to a particulate suspension can lead to the formation of a stable, space-spanning network of particles. The most dramatic consequence of such network formation is the transformation of a freely flowing suspension with a low viscosity into a paste-like material with strongly non-Newtonian rheology sometimes including a yield stress (Koos et al. 2012, Koos and Willenbacher 2011, 2012, McCulfor et al. 2011, Vankao et al. 1975). These results are easy to understand when the fluid that is added in a small quantity wets the particles. In that case, the added fluid forms menisci that bridge particles together and stabilize the space-spanning network, so that the pairwise interaction is dominated by attractive capillary forces. Incidentally, similar meniscus-bridging of particles has been long recognized in wet granular materials and is generally referred to as the *pendular state* (Iveson et al. 2002). On the other hand, when the minority fluid is non-wetting toward the particles, the reasons underlying network formation are less clear but seem to depend on clusters composed of several particles surrounding a single small drop (Koos and Willenbacher 2012). To our knowledge, similar capillary-induced structure formation has not been documented in filled polymers. If a capillary-induced network can indeed be formed successfully, this approach would offer a simple means of producing polymer-based composites featuring a three-dimensional percolating particle network.

The objectives of the present study are to explore the formation of capillary-induced particulate structures in multiphase polymer systems and, by extension, to gain deeper insights into morphological development in ternary systems in general. We investigate the structural and rheological consequences of adding a small amount of an immiscible polymer phase (referred to as the *minority polymer phase*) to a particle-filled polymer. In this research, the minority polymer phase almost completely wets the particles and hence is capable of forming a meniscus that can bridge the particles together. The first goal is to test if a pendular network can be realized by adding a minority wetting polymer phase to a filled polymer system, and if so, whether rheological properties can be used to detect the presence of this type of structure. The second goal is to test the effect of mixing conditions on structure formation. In the immiscible polymer blend literature, the mixing history is well-known to affect the morphology since the mechanisms that affect morphology development breakup or recoalescence of the dispersed phase, phase continuity, or morphological anisotropy are all directly related to the flow conditions during mixing (Jana and Sau 2004, Potschke and Paul 2003, Sundararaj et al. 1995, Sundararaj and Macosko 1995). In the present situation as well, it is reasonable to expect that without adequate mixing, the minority phase polymer may remain in the form of large inclusions that do not form a pendular network at all. Accordingly, the second objective is to compare different approaches for preparing the multiphase blends.

We show that addition of a minority wetting polymer induces a dual morphology consisting of both a pendular network of particles bridged by the wetting polymer as well as compact particle aggregates engulfed by the wetting polymer. The blend preparation method strongly influences the extent of compact particle aggregates, and with a suitable blending sequence, compact aggregation can be avoided altogether. Specifically, the drop size of the minority polymer phase is shown to be the key parameter that controls capillary aggregation. In the pendular network, interparticle contacts are maintained by meniscus-shaped capillary bridges, giving rise to significant sample elasticity (gel-like rheology). These "pendular gels" exhibit a yield stress behavior linked to their percolating nature. We show that the extent of network formation correlates well with the yield stress, thus providing a convenient method of verifying pendular network structures in future research.

Materials and methods

Materials

Polymers with Newtonian rheology are employed so that non-Newtonian behavior may be unambiguously attributed to the specific morphology of the multiphase system. The pair of immiscible polymers selected for this study is polyisobutylene (PIB, M_w~2,200 g/mol, ρ~0.908 g/mL, Soltex USA) and polyethylene oxide (PEO, M_w~20,000 g/mol, ρ~1.1 g/mL, Fluka). The PEO is semicrystalline at room temperature, and its melting point is close to 60 °C, whereas the PIB is liquid. Both PIB and PEO have a Newtonian flow behavior with a zero shear viscosity η_0 of 8 and 13 Pa.s (at 80 °C), respectively. The solid phase incorporated in the blends consists of spherical silica particles (SP, ρ~2 g/mL, Industrial Powder). These particles are polydisperse with a unimodal size distribution from 500 nm to 5 μm and the mean diameter is 2 μm. The PEO was rendered fluorescent using fluorescein sodium salt (F63377, Sigma Aldrich). PEO was dissolved in deionized water, and fluorescein was added at 0.1 wt.% of the PEO mass. The solution was homogenized using magnetic stirring for 1 h, and the deionized water was evaporated at 60 °C.

Blend preparation

The components were blended together using a MiniMax shear mixer (Maric and Macosko 2001), a device which consists of a cylindrical cup closed by an upper disk whose rotational speed is controlled by an external motor. Dispersive mixing capacity of the MiniMax was enhanced by the presence of three brass spheres in the mixer chamber (Maric and

Macosko 2001). The effective chamber volume was 4.9 mL, which allowed recovery of approximately 4 g of blended materials at the end of the mixing process. First, the silica particles were incorporated in the PIB by hand mixing using a spatula, and the binary mixture was further mixed in the MiniMax at 300 rpm for 2 min at room temperature. In a second step, the PEO was added in the MiniMax, and the mixing continued at 300 rpm for 2 min at 80 °C to ensure the melting of the PEO. Variations of this procedure were employed in order to investigate the influence of mixing conditions on the morphology of the blends. The samples are referred to as PIB/PEO/SP–*x*, where *x* refers to the mixing procedure as described in Table 1. Ternary blends of PIB/PEO/SP were prepared with a 77:3:20 weight ratio. Here, the PEO is used as the minority wetting polymer phase and is therefore present in much smaller proportion than the continuous polymer phase (PIB). In order to highlight the effect of the minority polymer phase addition, a control sample was prepared without any PEO. This binary blend of PIB/SP was prepared with an 80:20 weight ratio using the first step of mixing procedure A (see Table 1). After completion of the mixing process, each blend was sealed into a petri dish using parafilm and kept at 5 °C for 30 min in order to accelerate crystallization of the PEO phase (when present) and subsequently placed under vacuum overnight in order to remove the entrapped air bubbles from the bulk material.

Morphological characterization

Optical imaging of the blends was carried out using a confocal laser scanning microscope (Olympus FluoView 500) with ×40 (NA=1.30), ×60 (NA=1.40), and ×100 (NA=1.35) oil immersion objectives. Both differential interference contrast (DIC) and fluorescence modes were used. In addition to confocal imaging, the particulate structures formed by the SP with the PEO were imaged at higher magnifications using a scanning electron microscope (Philips XL30 FEG SEM). For this purpose, selective dissolution of the PIB matrix was achieved using octane, and the residual solid phase was transferred onto a Millipore filter paper (0.1 μm in pore size). Additional washing with octane was carried out several times in order to ensure complete removal of the PIB. After drying at room temperature, the filter paper was placed on adhesive carbon tape attached to a SEM stub, and the sample surface was metal-coated using a gold/palladium sputtering target (for 90 s at 40 mA). SEM images were acquired with a secondary electron detector.

Rheological measurements

Small-amplitude oscillatory shear, stress ramp, and steady shear flow experiments were performed using a TA Instruments AR2000 stress-controlled rheometer equipped with an air convection oven. Dynamic shear experiments were conducted with a cone and plate geometry (40-mm diameter, 1° cone angle, and 49-μm cone truncation gap). A homemade serrated parallel plate geometry (25-mm diameter, 1-mm gap) featuring a roughness of 500 μm was used for non-linear experiments in order to suppress wall slip effects (detection of the wall slip regime is detailed in the Supplementary Material). Frequency sweeps were carried out from 100 to 0.1 rad/s for a strain amplitude γ_0=0.05 % within the linear viscoelastic domain. Yielding behavior of the blends was determined by applying stress ramps from 6 to 6,000 Pa over 10 min. Steady-state flow curves were obtained for shear rates spanning from 10^{-2} to 10^{2} s^{-1} (the steady-state regime was typically achieved after five strain units for each considered shear rate). All rheological tests were conducted at 80 °C.

Results

Morphological and rheological changes induced by PEO addition

Blend morphologies for the PIB/SP and PIB/PEO/SP–A are shown in Fig. 1. A striking difference is observed between the binary and the ternary systems: the PIB/SP blend has the typical structure of a particle-filled polymer at low particle loading, with a rather homogeneous distribution of particles in the suspending matrix (Fig. 1a). In contrast, a highly heterogeneous structure is found in the presence of PEO (Fig. 1b). Indeed, silica particles appear very close to each other in the ternary system, forming a tortuous path with a highly branched nature across the PIB matrix. This branched structure is observed throughout the bulk of the sample. However, irregular-shaped particle aggregates with characteristic size of several tens of micrometers are also present in the ternary system, as shown in lower magnification images (Fig. 1c, d).

Table 1 Summary of the mixing procedures for PIB/PEO/SP ternary blends

Mixing procedure	First step	Second step
A	PIB/SP 300 rpm for 2 min at 25 °C	+PEO 300 rpm for 2 min at 80 °C
B	PIB/SP 300 rpm for 2 min at 25 °C	+PEO 500 rpm for 10 min at 80 °C
C	PIB/PEO 1,000 rpm for 10 min at 80 °C	+SP 500 rpm for 2 min at 80 °C
D	PIB/PEO 50 rpm for 2 min at 80 °C	+SP 500 rpm for 2 min at 80 °C

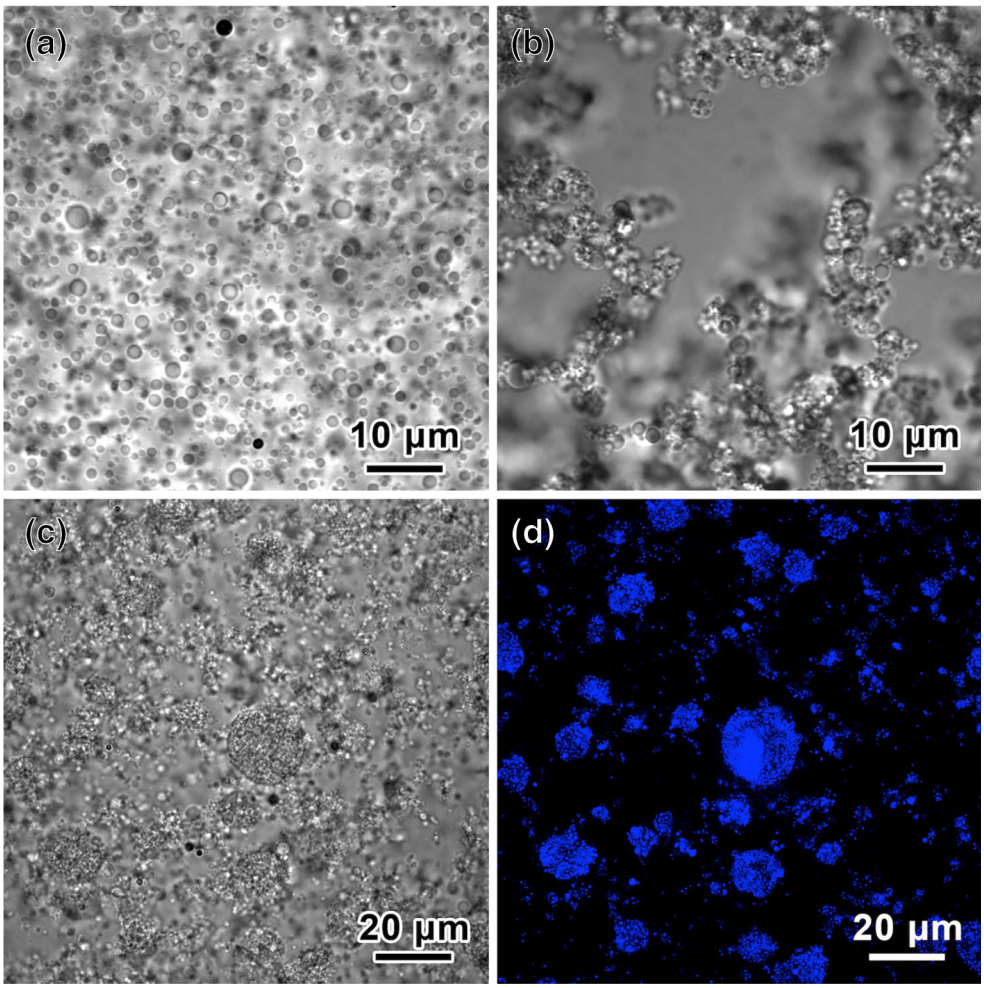

Fig. 1 Confocal micrographs of PIB/SP suspension (**a**) and PIB/PEO/SP–A pendular network (**b**). Lower magnification image of the PIB/PEO/SP–A sample (**c**) and corresponding fluorescent signal from the PEO (**d**), showing the coexistence of capillary-bridged network and capillary aggregates in the ternary blend. SP volume fraction is constant for both samples (ϕ_{SP}=0.1)

The fluorescence image (Fig. 1d) reveals the presence of PEO in two distinct types of location. Most obviously, the large aggregates show a strong fluorescent signal (blue color in Fig. 1d) indicating a high localization of PEO but also black voids which correspond to the non-fluorescent silica particles. The branched structures also show a fluorescent signal with much smaller typical size (in the micron–submicron range), indicating that the PEO also plays a role in holding the branched structures together. The supplementary data shows videos of dissolution of PIB using a selective solvent for a slightly different sample from Fig. 1, and the effect of added PEO on the aggregation behavior is readily apparent.

To illustrate these aggregated and branched structures more clearly, SEM was conducted after removal of PIB as described in the "Morphological characterization" section. A typical aggregate morphology is shown in Fig. 2a, where the aggregate appears densely packed with silica particles. We presume that the interstitial volume of such an aggregate is filled by the wetting polymer (PEO). Because of the presence of silica particles at their periphery, these aggregates feature a rough surface. This aggregate morphology is similar to the *capillary* state of saturation in wet granular materials (Iveson et al. 2002). Figure 2b on the other hand shows a detailed view of the branched structures, and at sufficiently high magnification, the PEO is seen to be present as capillary bridges between the particles (inset to Fig. 2b). This three-dimensional concatenation of silica particles, linked together by small PEO capillary bridges, is analogous to the *pendular* state of saturation of wet granular materials (Iveson et al. 2002). In the following, the branched structure is called *pendular network* and the drop-like PEO clusters containing packed silica particles are referred to as *capillary aggregates* for the sake of clarity.

In other multicomponent polymer systems such as polymer blends or filled polymers, the presence of large-scale structures is known to have a major influence on the rheology. Indeed, the rheological results can be used as a "signature" of the presence of a volume-spanning structure in co-continuous blends (Vinckier and Laun 1999, Vinckier and Laun 2001) or polymer-clay nanocomposites (Fornes et al. 2001, Krishnamoorti and Giannelis 1997, Lertwimolnun and Vergnes 2005, Solomon et al. 2001). Accordingly, it is of immediate interest to examine the rheological behavior of the ternary system. The frequency dependence of small-amplitude oscillatory shear experiments is depicted in Fig. 3

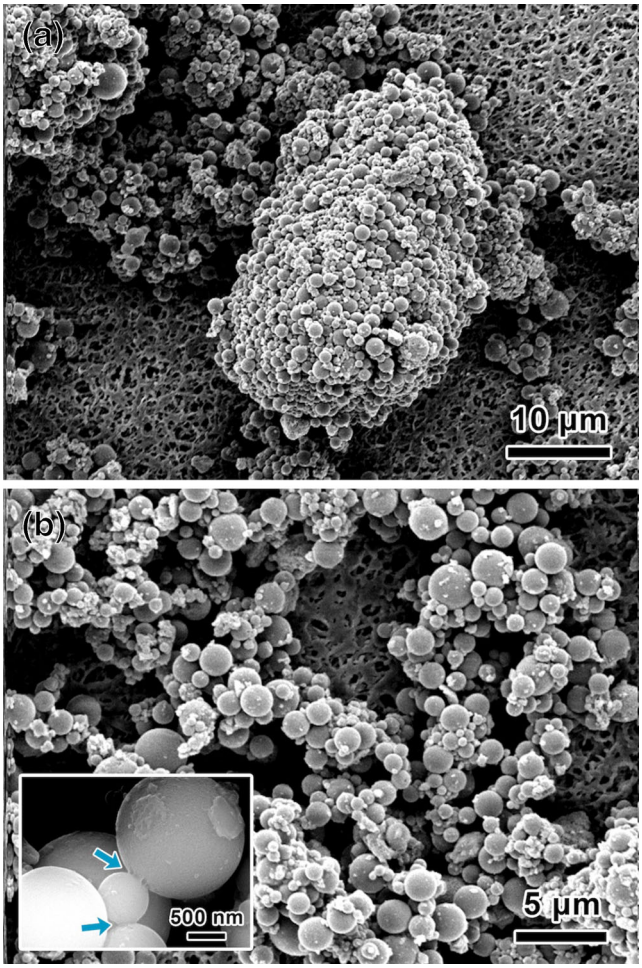

Fig. 2 SEM pictures of the PIB/PEO/SP–A blend after dissolution of the PIB matrix. **a** A capillary aggregate. **b** Pendular network. The *inset* shows a closer view of capillary bridges (*pointed out by the blue arrows*) between particles of different sizes in a branch of the pendular network

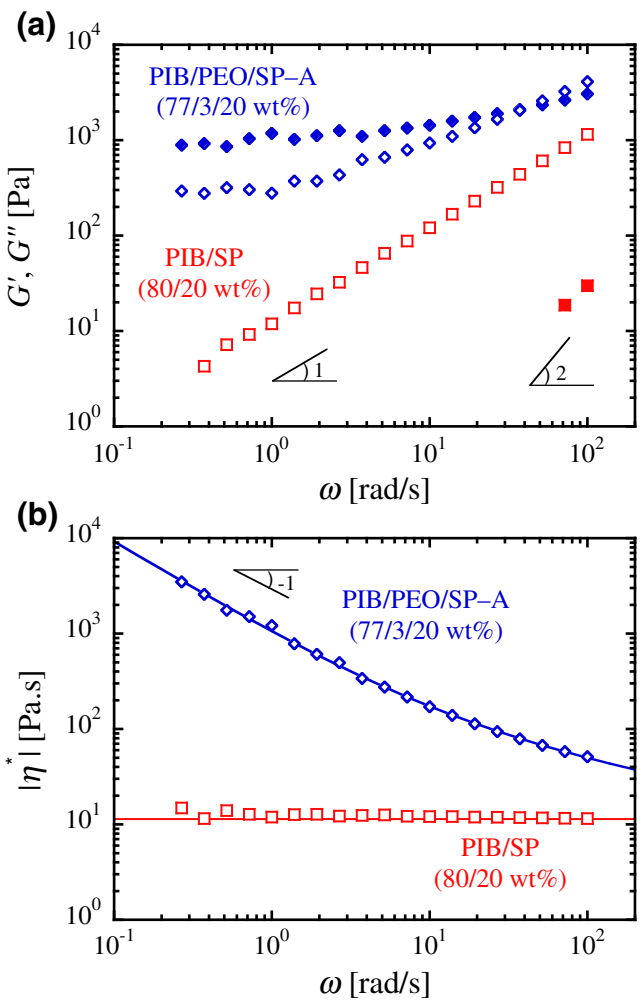

Fig. 3 Linear viscoelastic behavior of the PIB/SP binary blend and PIB/PEO/SP–A ternary blend. Angular frequency dependence of complex modulus (**a**) and complex viscosity (**b**). *Symbols* represent the data, whereas *continuous blue line* corresponds to the best fit using a Herschel–Bulkley type equation (see "Morphological and rheological changes induced by PEO addition") with σ_0=888 Pa, K=173 Pa.s^n, and m=0.69

for the PIB/SP binary blend and the PIB/PEO/SP–A ternary blend. The viscoelastic behavior of the binary system is very similar to the behavior of pure PIB: the complex viscosity is frequency-independent, and $G'<<G''$. Although G' is difficult to measure across a wide frequency range, the measurements suggest a nearly Maxwell-like dependence of the complex moduli ($G'(\omega)\sim\omega^2$ and $G''(\omega)\sim\omega$). On the other hand, the ternary system exhibits a strongly non-Newtonian behavior where no terminal flow regime is found at low frequencies. Instead, signature of a solid-like behavior ($G'>G''$ where both moduli become nearly frequency-independent at low frequencies) is observed. Importantly, the elastic modulus reaches a plateau value G'_p close to 10^3 Pa as the frequency decreases, and the complex viscosity can be fitted using a Herschel–Bulkley type equation $|\eta^*(\omega)| = \frac{\sigma_0}{\omega} + K\omega^{m-1}$ (continuous line in Fig. 3b). The volume fraction of silica particles ϕ_{SP} is 0.10 for both binary and ternary blends, far below the values of random loose and close packing fractions for monodisperse hard spheres (Scott 1960), and the slight increase in viscosity obtained for the binary system (compared to pure PIB) is in fair agreement with the Batchelor model for semi-dilute suspensions of hard spheres (Batchelor 1977). However, the significant increase in complex viscosity and the shear-thinning behavior observed for the ternary blend cannot be interpreted in the context of dilute hard-sphere suspensions. Indeed, these are landmark properties of large-scale percolating structures, and similar solid-like behavior was reported for other systems which feature a particulate network such as colloidal dispersions (Buscall et al. 1988, Piau et al. 1999, Pignon et al. 1998), polymer nanocomposites (Kim et al. 2010, Krishnamoorti and Giannelis 1997, Lertwimolnun and Vergnes 2005, Potschke et al. 2002, Solomon et al. 2001), reactive polymer blends (DeLeo and Velankar 2008), and more recently, for capillary suspensions based on small molecules fluids (Koos and Willenbacher 2011). Remarkably, the

apparent percolation of the ternary system is detected for a particle volume fraction ϕ_{SP} of only about 0.10, implying an even lower value for the percolation threshold, whereas the three-dimensional percolation threshold for monodisperse hard spheres is close to 0.30 (Isichenko 1992).

We attribute the non-terminal behavior in the low-frequency regime to the strong elastic contribution of the pendular network. The presence of compact capillary aggregates is less likely to contribute to the low-frequency solid-like rheology since these entities appear to be either isolated from the network or only loosely connected to it and do not form a volume-spanning cluster. Although the ternary blend displays shear-thinning, its complex viscosity values in the high-frequency regime are still significantly higher than the Newtonian viscosity of the binary blend (see Fig. 3b). This complex viscosity gap at higher frequencies may be attributable to the viscous contribution of both the pendular network and capillary aggregates in the ternary system.

The addition of PEO also has a significant effect on the non-linear rheology, as may be seen through stress ramp experiments. The shear stress dependence of the apparent viscosity of the binary and ternary blends is plotted in Fig. 4. The viscosity of the binary blend is found to be nearly constant during the ramp, whereas the ternary blend shows yielding and shear thinning as the stress increases. Furthermore, the final viscosity plateau observed at large stress for the ternary blend approaches the Newtonian viscosity of the binary suspension, suggesting a breakdown of the percolating structure in the ternary system. The microstructural nature of the breakdown is not yet known but may involve rupture of interparticle capillary bridges within the pendular network. This will be discussed further in the "Discussion."

These observations lead to the morphological picture of Fig. 5. Starting with a suspension of particles in the case of the binary system (Fig. 5a), the addition of the minority polymer phase leads to the simultaneous presence of capillary aggregates (Fig. 5b) and a pendular network (Fig. 5c). The pendular network is held by small concave-shaped PEO menisci bridging across particles. Due to the high wettability of the particles by the PEO (i.e., θ<<90° in Fig. 5), the PEO capillary bridge has a negative curvature and hence a negative Laplace pressure which results in an attractive force at the meniscus–solid interfaces (Cai and Bhushan 2008). This interparticle attraction stabilizes the pendular network. Finally, we note that Fig. 5b, c corresponds to two extremes, whereas in reality, the branched network may not be composed of purely pendular bridges. For instance, Fig. 5d illustrates a branched structure where the branches are few particles wide, which may be a more realistic representation of the branched structures seen experimentally. We emphasize that the schematic structures of Fig. 5b–d are favored only if the particles are almost fully wetted by the minority polymer. Here, the surface of silica particles is highly wettable by the PEO due to its polar groups along the backbone. Indeed, a previous study (Nagarkar and Velankar 2012) showed that unmodified colloidal silica particles can transfer from the PIB phase into the PEO phase during melt mixing, indicative of good wetting of the particles by the PEO. In contrast, particles with an organically modified surface were shown to remain trapped at the interface between PEO and PIB (Nagarkar and Velankar 2013, Nagarkar and Velankar 2012).

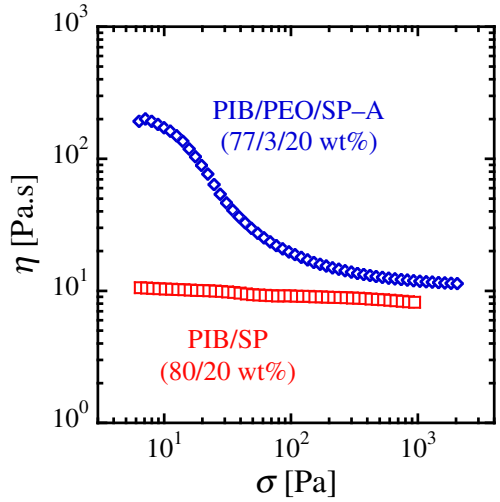

Fig. 4 Flow behavior of the PIB/SP binary blend and PIB/PEO/SP–A ternary blend during stress ramp experiments

Both capillary aggregates as well as pendular networks are expected to be thermodynamically stable under quiescent conditions. For instance, particle migration from a capillary aggregate to the matrix PIB requires energy of roughly $4\pi\alpha R^2$ where α is the interfacial tension between PEO and PIB, which is expected to be roughly 10^{-2} N m^{-1}. For a 1-micron radius particle, this energy is roughly 10^7 times of k_BT, i.e., thermal motion is unlikely to disrupt capillary aggregates. Similarly, a simple calculation shows that the surface work αA_{int} at the SP–PEO interface of a capillary bridge (where the area of the SP–PEO interface $A_{\text{int}} \sim 10^{-12}$ m^2) is approximately 10^7-fold superior to the thermal energy k_BT and thus that the pendular network is also a thermodynamically stable structure. Therefore, both structures are unlikely to get disrupted under quiescent conditions, and indeed, no structural changes were noted experimentally under quiescent conditions in the melt state. We may also comment on stability under flow conditions, e.g., during mixing. The capillary aggregates are composed of a high volume fraction of particles held together by a wetting polymer. Accordingly, this particle-in-PEO phase is likely to have a paste-like behavior with high viscosity below its yield stress (Coussot 2005, Heidlebaugh et al. 2014, Mewis and Wagner 2012). It is well-recognized in the polymer blending community that polymer phases with high viscosity or elasticity (as compared to the matrix) are difficult to breakup and disperse. Thus, once formed, capillary

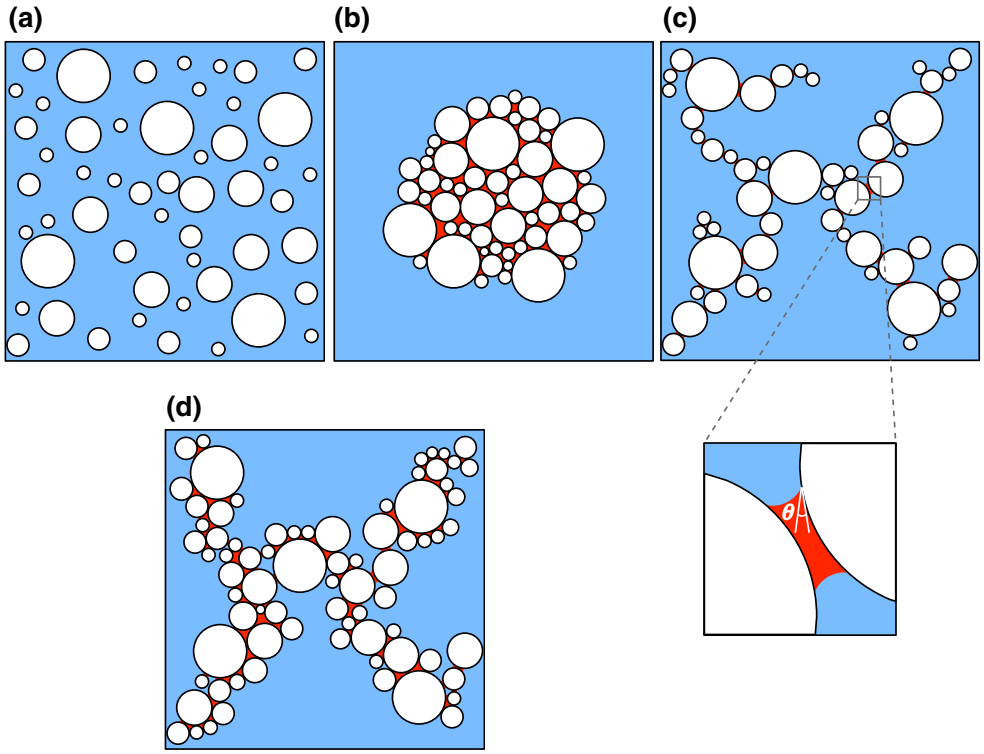

Fig. 5 Schematic morphologies of the blends: **a** silica particle suspension in the PIB matrix, **b** capillary aggregate, and **c** pendular network resulting from the addition of the minority polymer phase (PEO). The *zoom* in (**c**) shows a non-zero separation between particles only to better illustrate the contact angle. Pendular network structure with thicker branches is shown in (**d**). PIB in *blue*, PEO in *red*, and SP in *white*

aggregates are expected to be highly resistant to breakup. The pendular network on the other hand, being composed of large branches, likely undergoes continuous breakdown and reformation under mixing conditions. However, no coarsening of the pendular branches into capillary aggregates was observed when sheared under controlled conditions in the rheometer, suggesting that the loose structure of a pendular network does not coalesce into capillary aggregates under flow.

The presence of two very different types of structures in the ternary system raises questions about how these structures are formed by interaction between the minority polymer and the particles during melt mixing. More specifically, what controls whether the wetting fluid induces the formation of compact capillary aggregates or branched pendular network? Are capillary aggregates formed by advection of particles into PEO drops? Or are they formed by successive sticky collisions between PEO-coated particles? Furthermore, can rheology provide a convenient method for judging the extent to which particles form a percolating network due to capillary bridging? In the upcoming section, we address these questions by investigating the consequence of the melt-mixing procedure on the structure of the ternary system.

Influence of mixing conditions

As mentioned above, two simple processes of capillary aggregation during mixing can be considered. One is interphase particle transfer, where particles move from the polymer matrix to the inside of the minority polymer phase during mixing. This physical picture appears most intuitive if the PEO drop size exceeds the particles size significantly. The second possibility is the coalescence of PEO-wetted particles into successively larger aggregates; this seems more intuitive if the PEO wets the particles early during the mixing process. Accordingly, the mixing history of such ternary systems appears to be critical in determining the structure formation in the blend. To clarify this issue, we examined the effect of mixing procedure on the morphology of the ternary system.

Two main approaches were used to trace the influence of the mixing procedure on the resulting structure and rheology of the ternary blends. Each approach was carried out using two different processing conditions. Details of the four processing conditions can be found in Table 1. The final composition of every PIB/PEO/SP ternary blend sample is 77/3/20 wt.% regardless of the processing condition. The first approach (corresponding to mixing procedures A and B) aims at examining the importance of mixing intensity when the three components are simultaneously blended together. Briefly, the silica particles are pre-dispersed in the PIB matrix to ensure good dispersion and distribution of the particles, analogous to Fig. 1a. During the second step, the PEO is introduced, and the three components are subjected to mixing, either under low shear conditions (mixing procedure A) or high shear conditions (mixing procedure B). DIC images of the resulting morphologies are shown in Fig. 6. Clearly, the increase in mixing intensity leads to the formation of smaller and fewer capillary aggregates. However, the mechanism of capillary aggregation is still unclear at this point since shear-

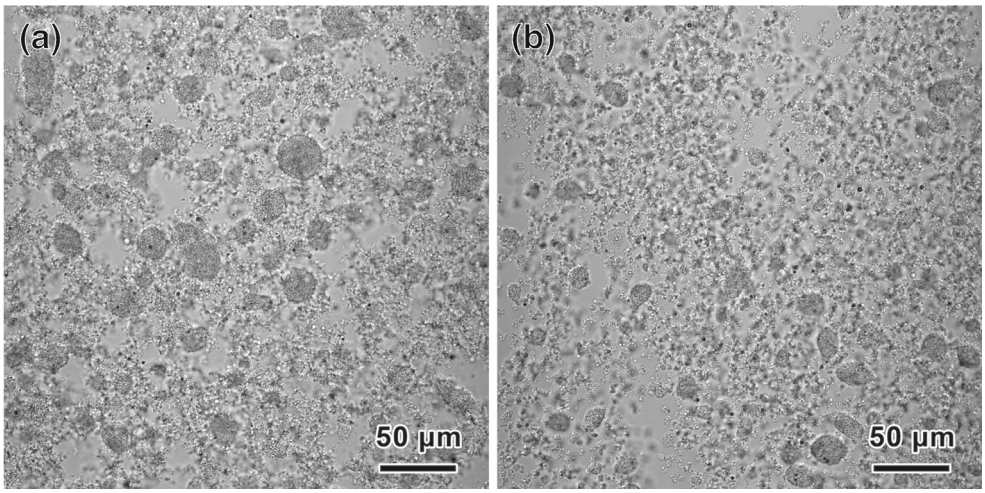

Fig. 6 Confocal micrographs (DIC) of PIB/PEO/SP ternary blends obtained with **a** mixing procedure A and **b** mixing procedure B

induced rupture of the PEO drops, and wetting of the silica particles by the PEO occur simultaneously during the second step.

Alternatively, we consider another pathway to assess the influence of mixing conditions by controlling the dispersion of the PEO phase prior to the addition of particles. For this purpose, we use a two-step mixing procedure where the PEO is first introduced into the PIB matrix and blended at either high or low intensity. The difference in PEO drop size distribution obtained for both conditions was examined by means of SEM after dissolution of the PIB matrix, as shown in Fig. 7a, b. Lower-intensity mixing leads to highly polydisperse drops, with a drop diameter ranging from a few microns up to approximately 40 μm, while much smaller drops are formed under intense mixing conditions (roughly 300 nm to 2 μm in diameter). It is noteworthy that the latter sizes are comparable to or smaller than the silica particle sizes. Starting from these two significantly different PEO drop size distributions, silica particles are added during the second step, and the three components are mixed under identical conditions (see Table 1 for details). In summary, two ternary blends are obtained with this approach: one sample made by adding particles to a fine dispersion of PEO drops in PIB (mixing procedure C) and another sample made by adding particles to a coarse dispersion of PEO drops in PIB (mixing procedure D). Optical images of these two samples are shown in Fig. 7c, d. A striking feature is the complete absence of capillary aggregates in the case of mixing procedure C (i.e., starting from small PEO drops) where only the pendular network is observed (see Fig. 7c). This absence of capillary aggregates was confirmed by further SEM observations (not shown). On the other hand, capillary aggregation occurred to some extent in the case of mixing procedure D (i.e., starting from large PEO drops). This suggests that capillary aggregation is not caused by an excess of PEO (i.e., more than necessary for the pendular network to form) but is rather related to the presence of large PEO drops that engulf the particles.

Finally, we examine the impact of mixing conditions on the rheology of ternary blends. Figure 8 shows the flow curves for the two extreme cases, i.e., the systems obtained by mixing procedures A (largest extent of capillary aggregates) and C (absence of capillary aggregates). The behavior of the other two samples lies between these two and has been omitted for clarity (these flow curves are shown in Fig. S2 of the Supplementary Data). All samples evince strongly non-Newtonian behavior characterized by shear thinning, with the viscosity leveling off to a plateau as the shear rate approaches 10^2 s^{-1}. We note that the viscosity values at low shear rate are affected by the mixing conditions, although all samples converge toward the same viscosity plateau at higher rate. The yield stress behavior can be well described by the Herschel–Bulkley model:

$$\sigma(\dot{\gamma}) = \sigma_y + k\dot{\gamma}^n \tag{1}$$

The yield stresses measured for the ternary blends obtained with the four mixing procedures (see Table 2) exhibit the following trend: *reduction in size and quantity of capillary aggregates leads to an increase in yield stress*. This supports the physical picture that the yield-like behavior is attributable to the pendular network with little or no contribution from the compact aggregates. Essentially, each silica particle is either trapped in a capillary aggregate or part of the pendular network. Therefore, when processing conditions help to reduce (or even eliminate) the formation of capillary aggregates, fewer particles get trapped in the aggregates and can join the pendular network, contributing to its strength and thus resulting in higher elasticity and higher yield stress of the ternary system. The trend found for the rheological behavior is thus related to the extent of capillary aggregation vs.

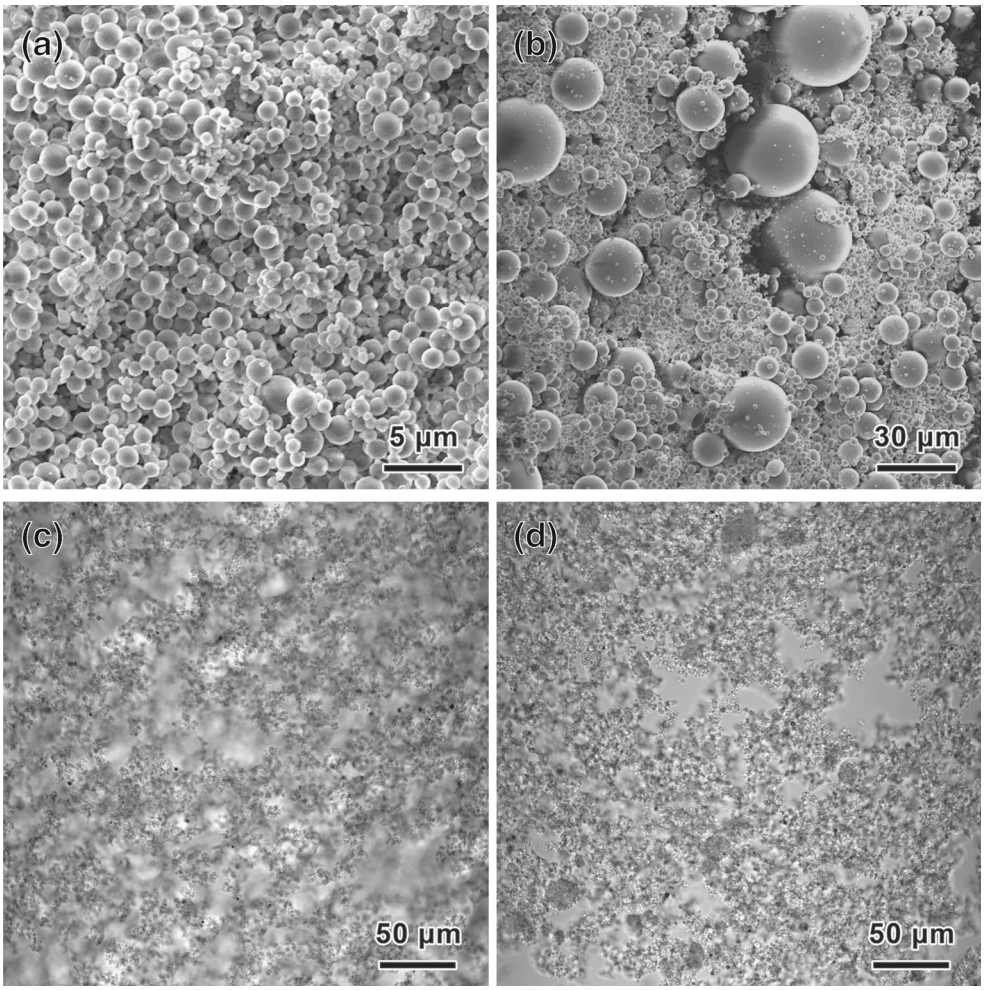

Fig. 7 SEM observations of PEO drops after mixing at **a** 1,000 rpm for 10 min and **b** 50 rpm for 2 min, and confocal micrographs (DIC) of PIB/PEO/SP ternary blends obtained with **c** mixing procedure C and **d** mixing procedure D

capillary bridging during the mixing process, and therefore, rheology may be used to gauge the extent of network formation.

Discussion

We will first discuss the experimental results presented in Figs. 6 and 7 to provide a physical picture for how aggregates form during mixing. These results suggest that capillary aggregates appear if the particles encounter PEO in the form of large drops during the mixing process. We propose that the size of the PEO dispersed phase during mixing influences the balance between capillary aggregation and meniscus bridging. This may be illustrated via two extreme cases of the relative size between drops and particles, as shown schematically in Fig. 9. In the case of low particle/drop size ratio, the particle can collide with the PEO phase during mixing, and due to the high wettability of the particles by the PEO, become engulfed by the PEO. By repeating this sequence, many more particles can enter the PEO drop, thus eventually forming a capillary aggregate (Fig. 9a). Since aggregates have a very high viscosity, they are likely to survive subsequent mixing even though some breakdown may still occur (Heidlebaugh et al. 2014). In contrast, if a particle collides with a much smaller PEO drop during mixing, the PEO is expected to spread on the particle. A collision with another particle can then result in the formation of a capillary bridge (Fig. 9b). Repetition of such a scenario can lead to the formation of a pendular network. The particle/drop size ratio thus appears as a major factor for the resulting morphology of the ternary system. Finally, we noted in the "Morphological and rheological changes induced by PEO addition" section that a purely pendular network and capillary aggregates are extreme cases, whereas a structure such as in Fig. 5d, with thicker branches, may be closer to the actual structure (e.g., Figs. 1b and 2b). Such thick branches may be formed if the capillary bridge between two particles is sufficiently large that other particles can join the meniscus (Heidlebaugh et al. 2014).

Next, we turn to a consideration of the structural breakdown of the network under flow conditions. One remarkable way to point this out is to compare the complex viscosity $|\eta^*(\omega)|$ in the linear viscoelastic regime against the steady

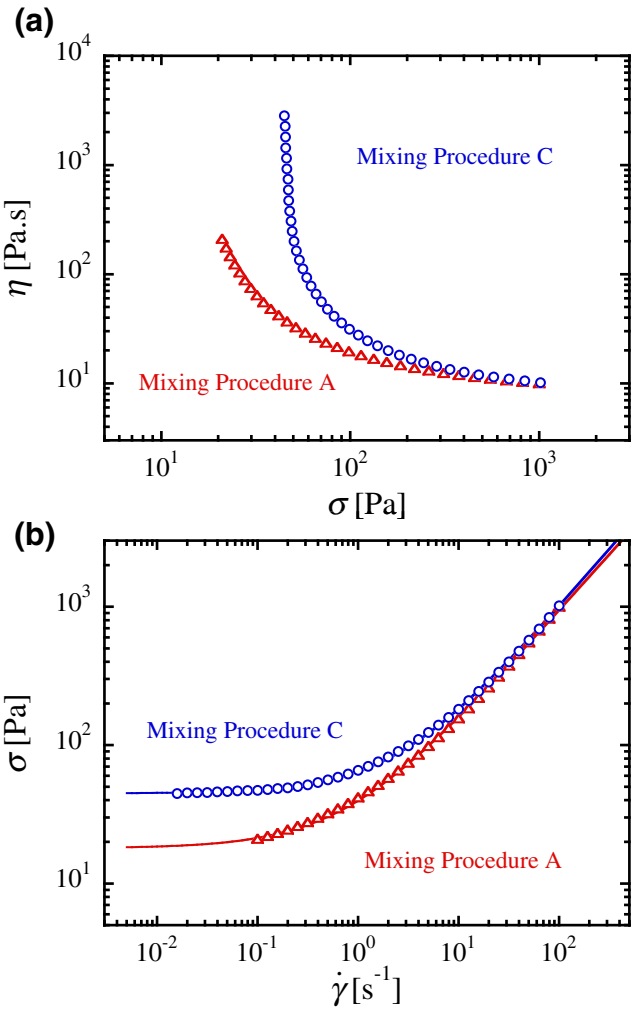

Fig. 8 Steady-state flow curves of the 77/3/20 ternary blend for the different mixing conditions. **a** Viscosity vs. stress and **b** stress as a function of shear rate. *Symbols* represent the data, whereas *continuous lines* correspond to the best fits using the Herschel–Bulkley model

shear viscosity $\eta(\dot{\gamma})$. For many simple fluids, including molten polymers, these two quantities agree very well with each other, an observation extensively known as the Cox–Merz rule (Cox and Merz 1958). This representation is shown in Fig. 10 for the PIB/SP binary system and the PIB/PEO/SP ternary blend prepared using mixing procedure C, in which capillary aggregates are completely absent. While the superposition principle holds true for the binary system, the presence of a percolated structure elicits the failure of the Cox–Merz rule in the case of the ternary system. This feature indicates that the three-dimensional network structure is perturbed under shear flow. An extended version of the Cox–Merz rule (Doraiswamy et al. 1991), which intend to reconcile the complex viscosity in linear and non-linear oscillatory experiments with the steady shear viscosity, was also found to be unsuccessful with our ternary system (graph not shown). It is noteworthy that this extended Cox–Merz rule was also found to be ineffective for polymer nanocomposites networks (Nazockdast et al. 2008, Rodlert et al. 2004). In the "Morphological and rheological changes induced by PEO addition" section, we suggested that such a shear-induced perturbation might be a disruption of the pendular network due to rupture of the capillary menisci bridging particles. We speculate that with increasing shear rate, the branched structures reduce in size analogous to the behavior of flocculated particulate suspensions (Larson 1999). Indeed, Supplementary Figure S2 shows that when the applied shear stress greatly exceeds the yield stress, the viscosity of all four samples levels off to a value approaching that of the binary PIB/SP mixture. This apparent convergence of the different ternary samples with the binary sample may indicate that large branched structures, which are the ones that contribute most to the high viscosity, do not survive at sufficiently high stress. The variations in viscosity at low rates are thus linked to the strength of the pendular network formed under different mixing conditions.

Finally, we note that even though the system studied here shares many similarities with corresponding small-molecule particle/oil/water systems, the high viscosity of molten polymers suggests that important differences are likely to appear in polymeric systems. Specifically, while the static structure of the ternary system may be well-described by capillary forces between the particles, under flow conditions when the menisci continually break and reform, the interparticle forces may be severely rate-dependent. This is because when particles move with respect to each other, the viscous forces increase sharply when the interparticle distance h reduces. For instance, for equal-sized particles near contact moving apart from each other, the viscous force is given by (Russel et al. 1992):

$$F_v = \frac{6\pi\eta_m\dot{\gamma}R^3}{2h} \tag{2}$$

where η_m is the viscosity of the fluid between the particles (i.e., the viscosity of the meniscus-forming PEO polymer). Thus, for particles in close contact, i.e., small h, the viscous forces can be extremely large. The attractive meniscus force

Table 2 Optimized values for the fitting parameters of the Herschel–Bulkley model

Blend	σ_y (Pa)	k (Pa.s^n)	n
PIB/PEO/SP–A	18.0	21.8	0.81
PIB/PEO/SP–B	28.1	21.7	0.83
PIB/PEO/SP–C	44.8	19.7	0.85
PIB/PEO/SP–D	40.0	20.6	0.84

*Fixing n=1 (equivalent to the Bingham model) decreases fitting quality (especially for the shear-thinning to Newtonian regime transition) but does not change σ_y significantly

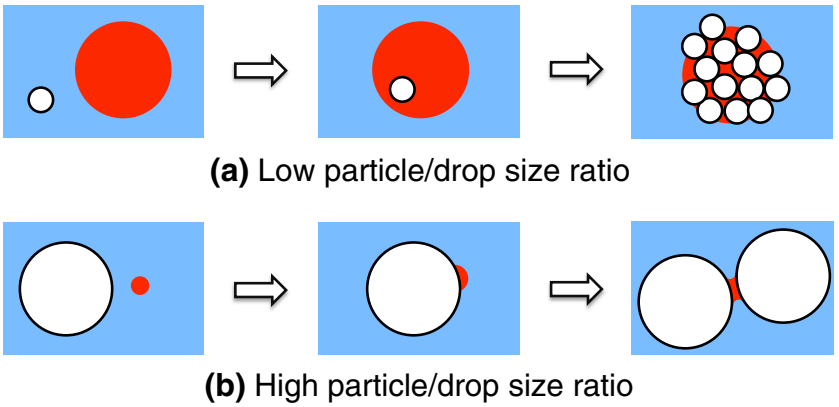

Fig. 9 Illustration of the influence of particle/drop size ratio on the association of SP with PEO during shear mixing. PIB in *blue*, PEO in *red*, and SP in *white*

on the other hand has a maximum value (when the particles are in contact) of (Israelachvili 1992):

$$F_m = 2\pi R\alpha\cos\theta \tag{3}$$

and the attractive meniscus force reduces toward zero as h increases. For our specific situation where the PEO wets the particles almost completely, θ is small, and hence, F_m is approximately $2\pi R\alpha$. The relative magnitude of viscous to capillary forces, which is a capillary number suitable for a meniscus geometry, can be expressed as:

$$Ca_{meniscus} = \frac{F_v}{F_m} = \frac{3}{2}\frac{\eta_m\dot{\gamma}R^2}{h\alpha} \tag{4}$$

Clearly, as the shear rate increases, viscous forces will become increasingly dominant. The relative magnitude of these two forces can be gauged using suitable values for the present experimental system: α=10^{-2} N m^{-1}, R=1 μm, and η_m=10 Pa.s. For $\dot{\gamma}$ =1 s^{-1}, $Ca_{meniscus}$ becomes on the order of 1 only when h is extremely small (about 1 nm). This suggests that in our current ternary polymer blends, the interparticle forces that resist meniscus breakup under flow conditions are dominated by interfacial tension forces. Yet, for many thermoplastics, the melt viscosity can be at least 100-fold higher than the PEO used here. In that case, $Ca_{meniscus}$ would be on the order of 1 even when h~100 nm, i.e., 10 % of the particle radius. In those cases, the meniscus breakup will likely be influenced by the viscosity of the wetting polymer and therefore by the deformation rate.

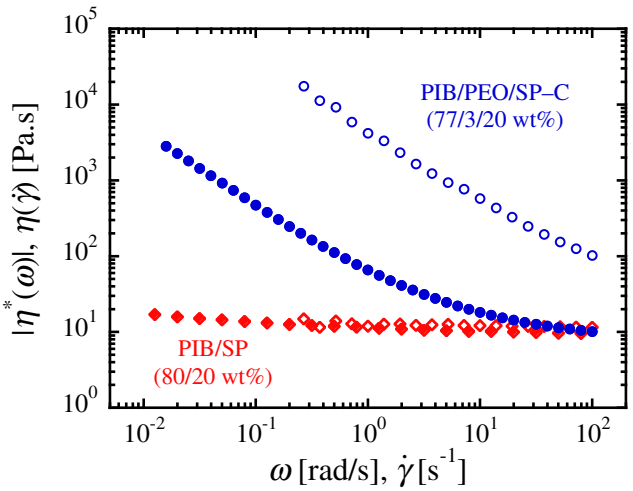

Fig. 10 Cox–Merz plots for the PIB/SP binary blend and PIB/PEO/SP–C ternary blend. *Empty symbols* for small-amplitude oscillatory shear and *filled symbols* for steady shear flow

Concluding remarks

We have examined the structural and rheological changes induced by the addition of a small amount of PEO to a mixture of silica particles in PIB by melt mixing. The silica particles are almost completely wetted by the PEO, which results in major structural changes. We show that capillary bridging of particles by PEO gives rise to the formation of a pendular network, a physical gel where particles are connected by small PEO menisci to create a three-dimensional tortuous path across the sample. Notably, this volume-spanning structure is formed at particle volume fraction of ~10 %, which is much lower than that needed for the percolation of hard spheres. On the other hand, high wettability of the particles by the minority PEO phase can also cause a portion of the particles to form closely packed capillary aggregates where the interstitial volume is filled by the PEO. We show that the extent of capillary aggregation strongly depends on the mixing conditions: the formation of capillary aggregates can be reduced or eliminated when the PEO drop size becomes comparable to or smaller than that of the particles size under mixing conditions.

These structural changes induced by addition of the wetting minority polymer phase cause massive changes in rheological behavior of the blends. Specifically, the ternary blends show solid-like behavior in small-amplitude oscillatory experiments, which is likely attributable to the elasticity of the

pendular network. Under steady flow conditions, the ternary blends show yield-like behavior and pronounced shear thinning, as well as violation of the Cox–Merz rule. Yielding is likely caused by the breakdown of the percolating structure under shear flow, where the rupture of PEO-mediated contacts eventually leads to Newtonian behavior at high shear rates. The rheological properties track microstructural differences between the various blends: the yield stress increases as the amount of compact capillary aggregates is reduced. This demonstrates that rheology can be used as a microstructural probe of the extent of pendular network formation in such systems.

Finally, qualitatively, this paper draws two chief conclusions, (1) Addressing the question posed in the "Introduction," we conclude that even a small amount of immiscible polymer can induce large changes in the microstructure of a particle-filled polymer and (2) Practically, this paper shows that capillary bridging of the particles by the addition of a small amount of wetting polymer can be an efficient way to reduce the percolation threshold of spherical particles filled into a polymer matrix.

Acknowledgments This research was supported by the National Science Foundation (NSF-CBET grant no. 0932901). We thank Dr. Jason Devlin, Morgan Jessup, and Mark Ross, Center for Biological Imaging at the University of Pittsburgh, for assistance with confocal imaging. We are grateful to Prof. George Petekedis, University of Crete, for pointing us to the literature on wall slip.

References

Batchelor GK (1977) The effect of Brownian motion on the bulk stress in a suspension of spherical particles. J Fluid Mech 83:97–117

Baudouin AC, Auhl D, Tao FF, Devaux J, Bailly C (2011) Polymer blend emulsion stabilization using carbon nanotubes interfacial confinement. Polymer 52:149–156

Binks BP, Horozov TS (2006) Colloidal particles at liquid interfaces. Cambridge University Press, Cambridge

Buscall R, Mills PDA, Goodwin JW, Lawson DW (1988) Scaling behaviour of the rheology of aggregate networks formed from colloidal particles. J Chem Soc Faraday Trans I 84:4249–4260

Cai S, Bhushan B (2008) Meniscus and viscous forces during separation of hydrophilic and hydrophobic smooth/rough surfaces with symmetric and asymmetric contact angles. Philos Trans A Math Phys Eng Sci 366:1627–1647

Cates ME, Clegg PS (2008) Bijels: a new class of soft materials. Soft Matter 4:2132

Chung H, Ohno K, Fukuda T, Composto RJ (2005) Self-regulated structures in nanocomposites by directed nanoparticle assembly. Nano Lett 5:1878–1882

Coussot P (2005) Rheometry of pastes, suspensions, and granular materials: applications in industry and environment. Wiley

Cox WP, Merz EH (1958) Correlation of dynamic and steady flow viscosities. J Polym Sci 28:619–622

DeLeo CL, Velankar SS (2008) Morphology and rheology of compatibilized polymer blends: Diblock compatibilizers vs crosslinked reactive compatibilizers. J Rheol 52:1385–1404

Doraiswamy D, Mujumdar AN, Tsao I, Beris AN, Danforth SC, Metzner AB (1991) The Cox–Merz rule extended: a rheological model for concentrated suspensions and other materials with a yield stress. J Rheol 35:647–685

Elias L, Fenouillot F, Majeste JC, Cassagnau P (2007) Morphology and rheology of immiscible polymer blends filled with silica nanoparticles. Polymer 48:6029–6040

Fenouillot F, Cassagnau P, Majeste JC (2009) Uneven distribution of nanoparticles in immiscible fluids: morphology development in polymer blends. Polymer 50:1333–1350

Fornes TD, Yoon PJ, Keskkula H, Paul DR (2001) Nylon 6 nanocomposites: the effect of matrix molecular weight. Polymer 42:09929–09940

Gubbels F, Jerome R, Teyssie P, Vanlathem E, Deltour R, Calderone A, Parente V, Bredas JL (1994) Selective localization of carbon-black in immiscible polymer blends—a useful tool to design electrical conductive composites. Macromolecules 27:1972–1974

Heidlebaugh SJ, Domenech T, Iasella SV, Velankar SS (2014) Aggregation and separation in ternary particle/oil/water systems with fully wettable particles. Langmuir 30:63–74

Herzig EM, White KA, Schofield AB, Poon WCK, Clegg PS (2007) Bicontinuous emulsions stabilized solely by colloidal particles. Nat Mater 6:966–971

Hong JS, Namkung H, Ahn KH, Lee SJ, Kim C (2006) The role of organically modified layered silicate in the breakup and coalescence of droplets in PBT/PE blends. Polymer 47:3967–3975

Horozov TS, Binks BP (2006) Particle-stabilized emulsions: a bilayer or a bridging monolayer? Angew Chem Int Ed 45:773–776

Huitric J, Ville J, Médéric P, Moan M, Aubry T (2009) Rheological, morphological and structural properties of PE/PA/nanoclay ternary blends: effect of clay weight fraction. J Rheol 53:1101

Isichenko MB (1992) Percolation, statistical topography, and transport in random media. Rev Mod Phys 64:961–1043

Israelachvili J (1992) Intermolecular and surface forces. Academic Press, Amsterdam

Iveson SM, Beathe JA, Page NW (2002) The dynamic strength of partially saturated powder compacts: the effect of liquid properties. Powder Technol 127:149–161

Jana SC, Sau M (2004) Effects of viscosity ratio and composition on development of morphology in chaotic mixing of polymers. Polymer 45:1665–1678

Kim H, Abdala AA, Macosko CW (2010) Graphene/polymer nanocomposites. Macromolecules 43:6515–6530

Koos E, Willenbacher N (2011) Capillary forces in suspension rheology. Science 331:897–900

Koos E, Willenbacher N (2012) Particle configurations and gelation in capillary suspensions. Soft Matter 8:3988–3994

Koos E, Johannsmeier J, Schwebler L, Willenbacher N (2012) Tuning suspension rheology using capillary forces. Soft Matter 8:6620–6628

Krishnamoorti R, Giannelis EP (1997) Rheology of end-tethered polymer layered silicate nanocomposites. Macromolecules 30:4097–4102

Larson RG (1999) Structure and rheology of complex fluids. Oxford University Press, New York

Lee MN, Mohraz A (2010) Bicontinuous macroporous materials from bijel templates. Adv Mater 22:4836–4841

Lee MN, Chan HK, Mohraz A (2012) Characteristics of pickering emulsion gels formed by droplet bridging. Langmuir 28:3085–3091

Lertwimolnun W, Vergnes B (2005) Influence of compatibilizer and processing conditions on the dispersion of nanoclay in a polypropylene matrix. Polymer 46:3462–3471

Maric M, Macosko CW (2001) Improving polymer blend dispersions in mini-mixers. Polym Eng Sci 41:118–130

McCulfor J, Himes P, Anklam MR (2011) The effects of capillary forces on the flow properties of glass particle suspensions in mineral oil. AIChE J 57:2334–2340

Mewis J, Wagner NJ (2012) Colloidal suspension rheology. Cambridge University Press, Cambridge

Nagarkar SP, Velankar SS (2012) Morphology and rheology of ternary fluid-fluid-solid systems. Soft Matter 8:8464–8477

Nagarkar S, Velankar SS (2013) Rheology and morphology of model immiscible polymer blends with monodisperse spherical particles at the interface. J Rheol 57:901–926

Nazockdast E, Nazockdast H, Goharpey F (2008) Linear and nonlinear melt-state viscoelastic properties of polypropylene/organoclay nanocomposites. Polym Eng Sci 48:1240–1249

Piau JM, Dorget M, Palierne JF, Pouchelon A (1999) Shear elasticity and yield stress of silica–silicone physical gels: fractal approach. J Rheol 43:305

Pickering SU (1907) Emulsions. Journal of the Chemical Society, Abstracts 91, 92:2001-2021

Pignon F, Magnin A, Piau J-M (1998) Thixotropic behavior of clay dispersions: combinations of scattering and rheometric techniques. J Rheol 42:1349

Potschke P, Paul DR (2003) Formation of co-continuous structures in melt-mixed immiscible polymer blends. J Macromol Sci Polym Rev C43:87–141

Potschke P, Fornes TD, Paul DR (2002) Rheological behavior of multiwalled carbon nanotube/polycarbonate composites. Polymer 43:3247–3255

Ramsden W (1903) Separation of solids in the surface-layers of solutions and 'suspensions' (observations on surface-membranes, bubbles, emulsions, and mechanical coagulation).—Preliminary account. Proc R Soc Lond Ser A Math Phys Eng Sci 72:156–164

Ray SS, Pouliot S, Bousmina M, Utracki LA (2004) Role of organically modified layered silicate as an active interfacial modifier in immiscible polystyrene/polypropylene blends. Polymer 45:8403–8413

Rodlert M, Plummer CJG, Leterrier Y, Månson J-AE, Grünbauer HJM (2004) Rheological behavior of hyperbranched polymer/montmorillonite clay nanocomposites. J Rheol 48:1049–1065, 1978-present

Russel WB, Saville DA, Schowalter WR (1992) Colloidal dispersions. Cambridge University Press

Scott GD (1960) Packing of spheres. Nature 188:908–911

Si M, Araki T, Ade H, Kilcoyne ALD, Fisher R, Sokolov JC, Rafailovich MH (2006) Compatibilizing bulk polymer blends by using organoclays. Macromolecules 39:4793–4801

Solomon MJ, Almusallam AS, Seefeldt KF, Somwangthanaroj A, Varadan P (2001) Rheology of polypropylene/clay hybrid materials. Macromolecules 34:1864–1872

Stancik EJ, Fuller GG (2004) Connect the drops: using solids as adhesives for liquids. Langmuir 20:4805–4808

Sundararaj U, Macosko CW (1995) Drop breakup and coalescence in polymer blends: the effects of concentration and compatibilization. Macromolecules 28:2647–2657

Sundararaj U, Dori Y, Macosko CW (1995) Sheet formation in immiscible polymer blends—model experiments on initial blend morphology. Polymer 36:1957–1968

Thareja P, Velankar SS (2007) Particle-induced bridging in immiscible polymer blends. Rheol Acta 46:405–412

Thareja P, Moritz K, Velankar SS (2010) Interfacially active particles in droplet/matrix blends of model immiscible homopolymers: particles can increase or decrease drop size. Rheol Acta 49:285–298

Van Puyvelde P, Velankar S, Moldenaers P (2001) Rheology and morphology of compatibilized polymer blends. Curr Opin Colloid Interf Sci 6:457–463

Vankao S, Nielsen LE, Hill CT (1975) Rheology of concentrated suspensions of spheres. 2. Suspensions agglomerated by an immiscible 2nd liquid. J Colloid Interface Sci 53:367–373

Vermant J, Cioccolo G, Nair KG, Moldenaers P (2004) Coalescence suppression in model immiscible polymer blends by nano-sized colloidal particles. Rheol Acta 43:529–538

Vermant J, Vandebril S, Dewitte C, Moldenaers P (2008) Particle-stabilized polymer blends. Rheol Acta 47:835–839

Vinckier I, Laun HM (1999) Manifestation of phase separation processes in oscillatory shear: droplet-matrix systems versus co-continuous morphologies. Rheol Acta 38:274–286

Vinckier I, Laun HM (2001) Assessment of the Doi-Ohta theory for co-continuous blends under oscillatory flow. J Rheol 45:1373–1385

Witt JA, Mumm DR, Mohraz A (2013) Bijel reinforcement by droplet bridging: a route to bicontinuous materials with large domains. Soft Matter 9:6773